Time-irreversibility and criticality in the motility of a flagellate microorganism

Kirsty Y. Wan[1, 2, *] and Raymond E. Goldstein[1, †]

[1] *Department of Applied Mathematics and Theoretical Physics, Centre for Mathematical Sciences, University of Cambridge, Cambridge, United Kingdom*

[2] *Living Systems Institute, University of Exeter, Exeter, United Kingdom*

(Dated: March 11, 2018)

Active living organisms exhibit behavioural variability, partitioning between fast and slow dynamics. Such variability may be key to generating rapid responses in a heterogeneous, unpredictable environment wherein cellular activity effects continual exchanges of energy fluxes. We demonstrate a novel, non-invasive strategy for revealing non-equilibrium control of swimming – specifically, in an octoflagellate microalga. These organisms exhibit surprising features of flagellar excitability and mechanosensitivity, which characterize a novel, time-irreversible '*run–stop–shock*' motility comprising forward *runs*, knee-jerk *shocks* with dramatic beat reversal, and long *stops* during which cells are quiescent yet continue to exhibit submicron flagellar vibrations. Entropy production, associated with flux cycles arising in a reaction graph representation of the gait-switching dynamics, provides a direct measure of detailed balance violation in this primitive alga.

In his *De Incessu Animalium*, Aristotle had thus described the walk of a horse [1]: "*the back legs move diagonally in relation to the front legs, for after the right fore leg animals move the left hind leg, and then the left foreleg, and finally the right hind leg.*" Since Aristotle, the control of locomotion in most animals is now understood to be enabled by central pattern generators [2], yet despite lacking a nervous system, certain primitive microeukaryotes can also actuate microscale analogues of limbs called cilia and flagella to produce swimming gaits akin to the trot and gallop of quadrupeds [3]. Likewise, these microorganisms are not restricted to a single gait but rather are capable of multiple: classic examples include the run and tumble of *E. coli* [4], the run-reverse-flick of *V. alginolyticus* [5], and the numerous escape gaits of the ciliate *P. tetraaurelia* [6]. Such heterogeneity of movement (in terms of speed, or directionality) is conserved across multiple species, and is crucial for effecting rapid responses within a dynamic and unpredictable environment [7].

To avoid the perpetual tendency toward disorder, living organisms take in free energy by consuming ATP, rendering the intracellular milieu a hub of activity whose non-equilibrium nature is traditionally quantified by invoking the thermodynamic fluctuation-dissipation theorem (FDT), e.g. by determining microrheological responses to weak external forcing [8]. At more macroscopic scales, microscopic breaking of detailed balance may be disguised or even partially restored. Inference of departure from equilibrium is further hampered by the absence of a generalized FDT, prompting the development of novel, non-invasive strategies rooted in the identification of phase-space currents [9, 10]. Here, we show for the first time how violation of detailed balance may be detected at the level of a free-living organism.

We consider "steady-state" motility control in the flagellate marine alga *Pyramimonas octopus* [11] (Fig. 1). *P. octopus* belongs to a fascinating group of unicellular algae bearing 2^k flagella, which substantiates a delicate interplay between passive fluid mechanics and active intracellular control in the coordination of multiple flagella [3]. Cells are oblong or rectangular in aspect (Fig. 1), with length ($17.05\pm1.74\ \mu m$) and width ($9.05\pm1.23\ \mu m$). Three gaits were consistently identified – the minimum number required for emergence of cycles or flux loops in a discrete representation. A forward-swimming *run* gait requiring synchronous, breaststroke coordination of diametrically opposed flagella pairs is interrupted by abrupt episodes involving dramatic changes in flagella beating, hereafter termed *shocks*. The third is a distinctive *stop* gait, which we found is associated with no cell body movement but yet minute flagellar oscillations.

Let us explore each of the three gaits in turn (Fig. 2a). Compared to bacteria, the larger size of these algae facilitates visualization – for details of experimental methods see Supplemental Materials (SM), allowing us to associate changes in flagellar beating unambiguously to gait transitions, and thence reorientation of swimming trajectories. When swimming freely, cells spin about their long axis, where the motion has a significant 3D component. However, by restricting to individuals traversing the focal plane we are able to observe the flagella distinctly. In

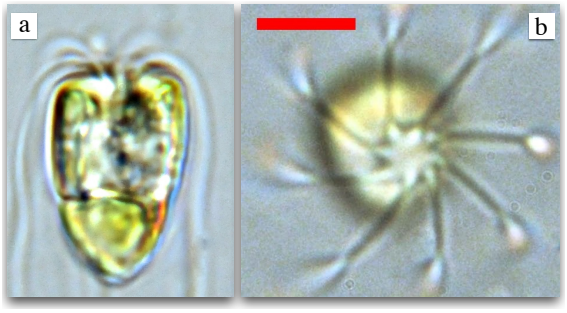

FIG. 1. (a) Side and (b) top views of *Pyramimonas octopus* (flagella spiraling clockwise viewed from above). Eyespot is visible as conspicuous orange organelle. (Scale bar: 5 μm.)

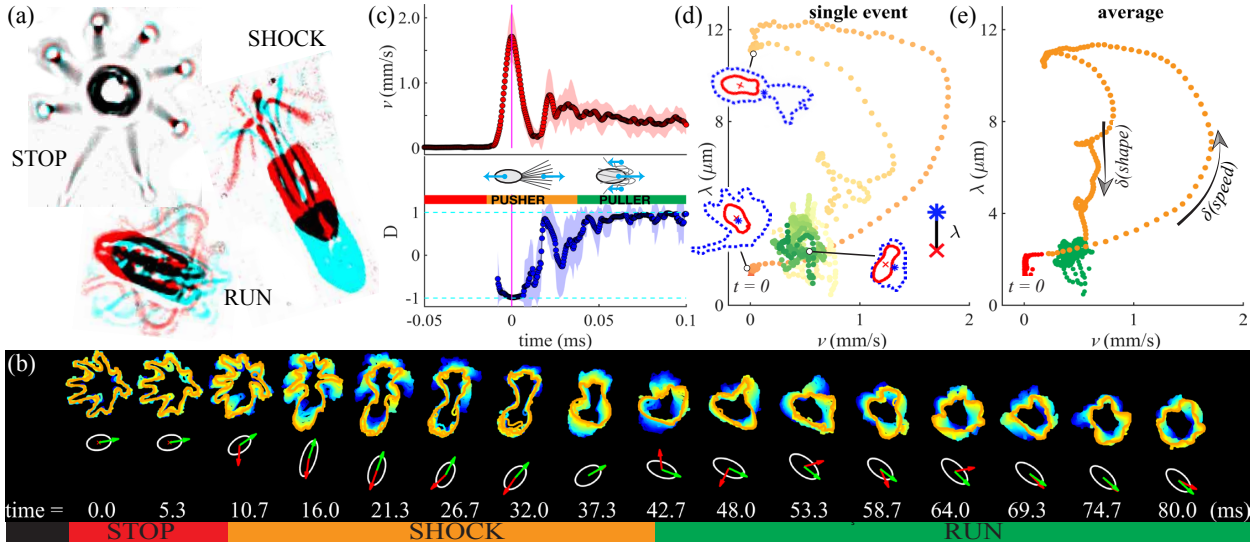

FIG. 2. (a) To visualize (stop, run, shock) gaits, pairs of video frames from different instants separated by (100, 10, 5) ms are merged, red: initial time, cyan: later time. (b) Dynamically changing flagellar waveforms result in cell reorientation, here, traced flagellar envelopes are displayed on coarse (10 ms) and fine (5 ms) timescales. (Cell body: ellipses, cell orientation $\hat{\mathbf{e}}_R$ & direction of motion $\hat{\mathbf{v}}$: green and red arrows.) (c) Transition from stop to run occurs via a shock, with rapid changes in speed v and alignment D ('pusher' to 'puller' transition, shaded region = 1 std). (d,e) Single and multicell phase-space trajectories.

a stereotypical gait sequence *stop* ⇀ *shock* ⇀ *run*: a cell initiates spontaneously a run from rest via a shock (Fig. 2b,c). Defining the instantaneous alignment $D = \hat{\mathbf{v}} \cdot \hat{\mathbf{e}}_R$ between the swimming direction $\hat{\mathbf{v}}$ and the cell body axis $\hat{\mathbf{e}}_R$, the puller-like run ($D = 1$) may be distinguished from the pusher-like shock ($D = -1$), during which all flagella are transiently thrown in front of the cell body (Fig. 2a). Concomitantly, the beat pattern also transitions from a bilateral ciliary to an undulatory flagellar beat [12]. Averaged over 10 cells, the translational speed rises rapidly from zero to a maximum of $1,712 \pm 392$ μm/s, but relaxation to a mean run speed of 428 ± 64 μm/s takes ~ 0.05 s. To separate flagellar motion from body orientation, we track two dynamically morphing boundaries that are delineated by image intensity: an inner one for the cell body, and an outer one exterior to the flagella (SM). The length $\lambda(t) = \left\| \sum_{\mathbf{x}\in\mathcal{B}\setminus\mathcal{A}} \mathbf{x}/|\mathcal{B}\setminus\mathcal{A}| - \sum_{\mathbf{x}\in\mathcal{A}} \mathbf{x}/|\mathcal{A}| \right\|$, measures the physical separation between the flagella and cell body proper, where $||\cdot||$ is the Euclidean norm, $|\cdot|$ the cardinality of a set, and $\mathcal{A}$, $\mathcal{B}$ are pixels interior of the inner and outer boundaries respectively.

Naturally, cells at rest exhibit minimal shape fluctuations. In Fig. 2d, the three gaits (sampled respectively at instants $t = 33$, 79, and 211 ms), localize to specific regions of phase-space. Trajectory bifurcations from stops to runs via shocks appear as loops with two distinct branches, one involving rapid changes in *speed*, the other in *shape* (Fig. 2e). To estimate the transition probabilities between gaits, we implemented a continuous time Markov model, using instantaneous speed v to automate a three-state gait discretization from digitized tracks (Fig. 3a). The state variable $X(t)$ takes the values $\{0 = \text{stop},\ 1 = \text{run},\ 2 = \text{shock}\}$. States are positive recurrent and the process is irreducible. The Markov assumption is general, and well-supported empirically by measurements of waiting time distributions between states. The transition rate matrix $Q = \{q_{ij}\}$, defined by $q_{ij} = \lim_{\Delta t\to 0} \mathcal{P}(X(\Delta t) = j | X(0) = i)/\Delta t$ for $i \neq j$ and $q_{ii} = -\sum_{j\neq i} q_{ij}$, expressed in units of s^{-1}, was estimated to be (full details see SM):

$$Q = \begin{array}{c} \\ \textit{stop} \\ \textit{run} \\ \textit{shock} \end{array} \begin{array}{c} \begin{array}{ccc} \textit{stop} & \textit{run} & \textit{shock} \end{array} \\ \begin{bmatrix} -0.132 & 0.008 & 0.124 \\ 0.281 & -1.330 & 1.049 \\ 0 & 19.77 & -19.77 \end{bmatrix} \end{array}. \quad (1)$$

In total, $\mathcal{O}(10^4)$s of cumulative recordings (individual track durations $0.5 - 80$ s) were analysed, from which $1,377$ distinct pairwise transitions were obtained from 233 cells. Expected waiting times are obtained from diagonal entries $-1/q_{ii}$, stop: 7.60 ± 0.75 s, run: 0.75 ± 0.03 s, shock: 0.05 ± 0.002 s (uncertainties are standard errors). The model predicts a unique equilibrium distribution $\pi(\text{stop}, \text{run}, \text{shock}) = (0.6666, 0.3126, 0.0208)$. Moreover, $\{\pi_i\}$ is in good agreement with estimated relative dwell times of (68.6%, 30.8%, 0.6%) in each of (stop, run, shock) states, as determined via a histogram of swimming speeds (Fig. 3b). The latter method uses a larger dataset which additionally includes tracks with no transitions, and is subjective in choice of cut-off (here, stop: $0 \leq v \leq 40$, run: $40 \leq v \leq 500$, shock: $v \geq 500$ μm/s).

While run ⇌ shock bifurcations occur readily, the direct reaction shock ⇀ stop is never observed. This

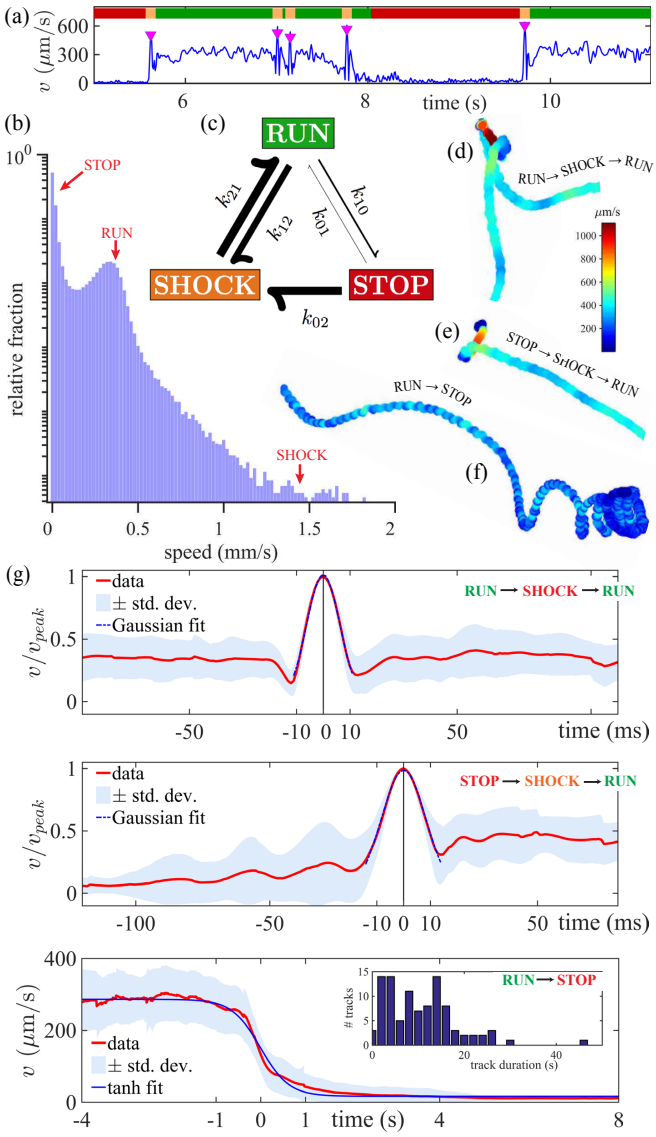

FIG. 3. (a) Single-cell motility is partitioned into three states (0: stop, 1: run,. 2: shock), according to instantaneous speed $v(t)$. Shocks are denoted by downward triangles. (b) Probability density distribution of speeds (log-scale) reveal dwell times in each state. (c) Permissible gait transitions are indicated by arrows (weighted by rates k_{ij}). (d)-(f) Sample trajectories for characteristic transition sequences. (g) Superimposed and averaged swimming speeds exhibit pulse-like maxima during shocks, but much slower decay during run $\rightharpoonup$ stop transitions. Inset: histogram of track durations.

continuous time process admits an embedded Markov chain $\{k_{ij}, i \neq j\}$ representing the probability of $i \to j$ transitions conditioned on discrete 'jump times' analogous to chemical reaction rates. Here, $k_{ii} = 0$ (no self-transitions), $\sum_j k_{ij} = 1$, $\forall i$. We find $k_{01} = 0.0582, k_{02} = 0.9418, k_{10} = 0.2112, k_{12} = 0.7888, k_{20} = 0$ and $k_{21} = 1.0000$ (Fig. 3c). Evidently, the chain is not reversible, violating detailed balance (as in the Kolmogorov flux criterion: $k_{01}k_{12}k_{20} \neq k_{02}k_{21}k_{10}$). Circulation balance is associated with entropy production and free-energy dissipation. From the steady state master equation $\dot{P}_i(t) = \sum_j (p_i k_{ij} - p_j k_{ji}) = 0$, with $p_i = \pi_i$, we define an entropy production rate $\dot{S}$ characterizing the difference between forward and time-reversed entropies [13]

$$\langle \dot{\mathcal{S}} \rangle = \frac{1}{2} \sum_{i \neq j} J_{ij} A_{ij} \geq 0 \tag{2}$$

from fluxes $J_{ij} = \pi_i k_{ij} - \pi_j k_{ji}$ and conjugate forces A_{ij},

$$A_{ij} = \begin{cases} \ln\left(k_{ij}/k_{ji}\right) & \text{if reversible} \\ \ln\left(k_{ij}(\pi_j T_{\max})\right) & \text{if irreversible .} \end{cases} \tag{3}$$

(Here, "irreversible" reactions are associated with rates $(\pi_j T_{\max})^{-1}$, where $T_{\max} = 78.17s$ is the maximum single-track duration.) We find $\langle \dot{\mathcal{S}} \rangle = 0.249$. $\dot{\mathcal{S}}$ *quantifies* the lack of detailed balance in the non-equilibrium steady state, and its modulation by environmental factors [14]. Thus, we have identified flux cycles in a single-cell motility strategy, which results in macroscopic violation of free Brownian diffusion, without neither the need for gait-transition rates to vary in space (e.g. bacterial run-and-tumble chemotaxis [15]), nor the introduction of spatially asymmetric obstructions (e.g. funnel ratchets) [16].

Gait-switching changes the morphology of trajectories. We zoom in Figs. 3d-f on three primary sequences allowable by Fig. 3c: run $\rightharpoonup$ shock $\rightharpoonup$ run, stop $\rightharpoonup$ shock $\rightharpoonup$ run, and run $\rightharpoonup$ stop. Typically of photosynthetic unicells [17], forward swimming is helical with a variable pitch superimposed onto self-rotation. Tracks comprise low-curvature portions due to runs, and sharp turns due to rapid conversion of flagellar beating and transient reversals during shocks. Runs decelerate to full-stop by sequentially deactivating *subsets of flagella* (see SM), producing a torque imbalance which gradually increases track curvature (Fig. 3f). Two disparate timescales are evidenced: an ultrafast, millisecond timescale for bifurcations to or from shocks, and a slower one for entry into stop states. The former is reminiscent of neuronal spiking while the latter is akin to decay of leakage currents. For the first two sequences (Fig. 3g), the mean is well fit to a sharply peaked Gaussian ($\sigma = 8.6$ ms, 11.6 ms respectively), whereas run to stop conversions follow a switch-like tanh profile with relaxation time $\tau = 640$ ms. The true maximum speed reached during shocks is likely even higher, since our imaging platform limits us to 2D projections of the motion.

This timescale separation is apparent in the stop gait, not previously characterized in the motility repertoire of algae. Here, a cell can remain stationary for minutes, yet restart swimming in tens of milliseconds (SM). Surprisingly, negligible cell body motion (with subpixel variance in centroid displacement: $\sigma_{\delta C} = 0.0253$ μm) is coupled with significant flagellar activity (O(1) μm fluctuations),

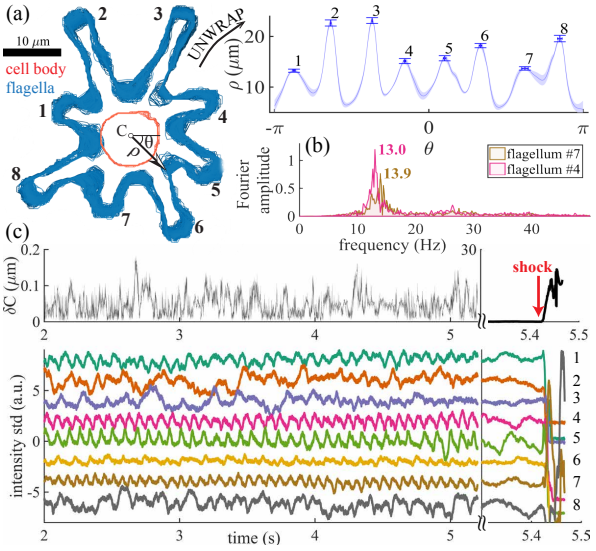

FIG. 4. (a) Cell and flagellar boundaries are digitized from successive frames and superposed during the stop gait (shaded region = one std. dev.). The flagella envelope exhibits correlated, μm-fluctuations (inset). (b) Individual flagella display robust oscillations. (c) Centroid fluctuations are sub-pixel and random, yet flagella tips oscillate until all 8 flagella bifurcate simultaneously to full-amplitude beating (shock).

and even small-amplitude oscillations (Fig. 4). This novel, highly-unusual vibrational mode may be related to hyperoscillations observed in reactivated sperm flagella, wherein noisy dynamics originate from oscillations of individual dyneins [18]. At onset of stop $\rightharpoonup$ shock transitions, the emergence of global limit-cycle beat oscillations is Hopf-like (Fig. 4) – occurring simultaneously in all 8 flagella.

Flagellar excitability in this organism is further evidenced by an acute mechanosensitivity, wherein shocks are induced by external stimuli – even contact with one flagellum (SM). These stimulated shocks are identical in morphology and dynamics to spontaneous (noise-induced) shocks. Fig. 5(a) shows a moving cell colliding with a cell at rest: contact is made multiple times but a shock is only triggered in cell 2 for a large enough perturbation. The required contact force $F = 3EI \cdot \delta/L^3$ is estimated from the tip deflection δ. For a non-beating flagellum with bending rigidity $EI = 840$ pNμm^2 [19], we find fail (no shock) when $F \lesssim 3.0$ pN, and success (shock) for $F \gtrsim 6.6$ pN. For multiple such collision events, we measured a O(10)ms signal transduction from the distal point of contact to flagellar response. Thus, shocks not only effects reorientation during swimming [20], but also enables ultrafast escape from predators or obstacles upon direct contact. Physiologically this may be related to the escape responses of *Chlamydomonas* and *Spermatozopsis* (which last much longer (0.2 – 1.0 s) and do not occur spontaneously, requiring instead strong light or mechanical triggers [21, 22]).

In summary, *P. octopus* is a microswimmer capable of robust behavioral stereotypy and responsiveness in the absence of neuronal control of the kind pertaining to animal models such as *D. melanogaster* or *C. elegans* [23, 24]. The run-stop-shock motility herein presented is a significant departure from known strategies such as the two-state *E. coli* run-and-tumble [4], or its sister eukaryotic version exhibited by the freshwater alga *C. reinhardtii* [25–27], and different still from alternatives such as the run-reverse-flick [5, 28]. Instead, we showed that gait-switching in *P. octopus* solicits total conversion of beating along the flagellar axoneme proper (Fig. 2a), in which *run*, *shock*, and *stop* gaits are coincident with the three major modes of eukaryotic flagella (*ciliary, flagellar, and quiescent*) [12]. This contrasts with classical gait-switching mechanisms reliant on a basal rotor or flagellar hook (as in bacteria), or on modulation of flagellar synchrony (as in *C. reinhardtii*). Thus, *P. octopus* is ideally suited for examining bifurcations between different modes in the *same* organelle.

By ascribing the observed motility patterns to a tripartite repertoire we were able to shed new light on the physiology of gait control in flagellates, revealing its strongly non-equilibrium character. Here, the breaking of detailed balance exposes an inherent temporal irreversibility in the flagellar control mechanism, adding further complexity to the need to enact time-irreversible beat patterns to overcome Stokes reversibility [29], meanwhile also consuming chemomechanical energy. We showed that a single, stereotypical run $\rightharpoonup$ stop $\rightharpoonup$ shock cycle elicits two timescales separated by two orders of magnitude, corresponding to rapid activation (forward reaction) but slow deactivation (backward reaction) of motility. Finally, our analyses suggest that active motility resides at criticality, instantiated by the phenomenon that quiescent flagella exhibit robust small-amplitude vibrations which bifurcate to full-amplitude oscillations when induced by noise or by weak mechanical forcing. Each flagellum, operating

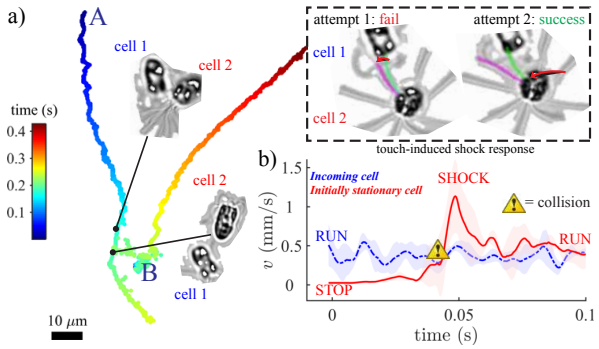

FIG. 5. (a) Acute flagellar mechanosensitivity: mechanical contact with only one flagellum is sufficient to trigger a shock given enough forcing (inset). (b) Sequence of changes in swimming speed averaged over four sample cell-cell collisions - in each case between a moving cell and a stationary cell.

far from equilibrium, executes highly nonlinear responses and large phase space excursions (Fig. 2a). These results have significant implications for modeling and understanding of beat emergence [30, 31] and dynein motor coordination in eukaryotic cilia and flagella [32–34].

Criticality and excitability are hallmarks of nonequilibrium activity, which may promote biological sensitivity (c.f. chemotaxis [35], hair cells of the inner ear [36]). We found *P. octopus* flagella to be more reactive to noise and mechanical perturbations compared to other species such as *C. reinhardtii* [37–39]. Its heightened sensitivity may result from adaptation to a unique benthic habitat in which rapid signal transduction is critical for avoiding physical obstacles (e.g. sand grains), or predation. In more advanced phyla, cilia and flagella continue to fulfill key sensory and motile functions, switching between neurally controlled oscillatory/non-oscillatory states in ctenophores [40], and generating nodal flows for embryonic symmetry breaking [41]. Thus, in this little-known, billion-year old unicellular marine alga, we may have found an evolutionary precedent for these highly-evolved and conserved functionalities.

Financial support is acknowledged from Magdalene College, Cambridge through a Junior Research Fellowship (KYW), and Senior Investigator Awards 097855MA and 207510/Z/17/Z from the Wellcome Trust (REG). We thank Robert G. Endres and Eric Lauga for discussions.

* K.Y.Wan2@exeter.ac.uk
† R.E.Goldstein@damtp.cam.ac.uk

[1] Aristotle. Parts of Animals. Movement of Animals, Progression of Animals, Trans. A.L. Peck & E.S. Forster, Loeb Classical Library 323 (Harvard University Press, Cambridge, MA 1961).
[2] K. G. Pearson, Annu. Rev. Neurosci. **16**, 265 (1993).
[3] K. Y. Wan and R. E. Goldstein, Proc. Natl. Acad. Sci. USA **113**, E2784 (2016).
[4] H. C. Berg and D. A. Brown, Nature **239**, 500 (1972).
[5] K. Son, J. S. Guasto, and R. Stocker, Nat. Phys. **9**, 494 (2013).
[6] A. Hamel, C. Fisch, L. Combettes, P. Dupuis-Williams, and C. N. Baroud, Proc. Natl. Acad. Sci. USA **108**, 7290 (2011).
[7] R. M. Colwill and R. Creton, Rev. Neuro. **22**, 63 (2011).
[8] M. Guo, A. J. Ehrlicher, M. H. Jensen, M. Renz, J. R. Moore, R. D. Goldman, J. Lippincott-Schwartz, F. C. Mackintosh, and D. A. Weitz, Cell **158**, 822 (2014).
[9] F. Gnesotto, F. Mura, J. Gladrow, and C. P. Broedersz, arxiv: 1710.03456 (2017).
[10] C. Battle, C. P. Broedersz, N. Fakhri, V. F. Geyer, J. Howard, C. F. Schmidt, and F. C. MacKintosh, Science **352**, 604 (2016).
[11] O. Moestrup and T. Hori, Protoplasma **148**, 41 (1989).
[12] We take "ciliary" to mean the large-amplitude asymmetric beat exhibited by most cilia (e.g. epithelial) where the beat cycle partitions into distinct power and recovery stroke phases, and"flagellar" to mean the symmetric undulatory beat of sperms.
[13] J. Schnakenberg, Rev. Mod. Phys. **48**, 571 (1976).
[14] K. Y. Wan and R. E. Goldstein, preprint (2018).
[15] M. E. Cates, Rep. Prog. Phys. **75**, 042601 (2012).
[16] G. Lambert, D. Liao, and R. H. Austin, Phys. Rev. Lett. **104**, 168102 (2010).
[17] G. B. Witman, Trends Cell. Biol. **3**, 403 (1993).
[18] S. Kamimura and R. Kamiya, Nature **340**, 476 (1989).
[19] G. Xu, K. S. Wilson, R. J. Okamoto, J. Y. Shao, S. K. Dutcher, and P. V. Bayly, Biophys. J. **110**, 2759 (2016).
[20] F. Peruani and L. G. Morelli, Phys. Rev. Lett. **99**, 010602 (2007).
[21] R. Eckert, Science **176**, 473 (1972).
[22] K. Fujiu, Y. Nakayama, A. Yanagisawa, M. Sokabe, and K. Yoshimura, Curr. Biol. **19**, 133 (2009).
[23] G. J. Berman, W. Bialek, and J. W. Shaevitz, Proc. Natl. Acad. Sci. USA **113**, 11943 (2016).
[24] G. J. Stephens, M. B. de Mesquita, W. S. Ryu, and W. Bialek, Proc. Natl. Acad. Sci. USA **108**, 7286 (2011).
[25] M. Polin, I. Tuval, K. Drescher, J. P. Gollub, and R. E. Goldstein, Science **325**, 487 (2009).
[26] J. S. Guasto, K. A. Johnson, and J. P. Gollub, Phys. Rev. Lett. **105**, 168102 (2010).
[27] K. Y. Wan, K. C. Leptos, and R. E. Goldstein, J. R. Soc. Interface **11**, 20131160 (2014).
[28] K. M. Taute, S. Gude, S. J. Tans, and T. S. Shimizu, Nat. Comm. **6**, 8776 (2015).
[29] R. Golestanian and A. Ajdari, Phys. Rev. Lett. **100**, 038101 (2008).
[30] P. V. Bayly and K. S. Wilson, J. R. Soc. Interface **12**, 20150124 (2015).
[31] D. Oriola, H. Gadelha, and J. Casademunt, Roy. Soc. open sci. **4**, 160698 (2017).
[32] C. B. Lindemann, Journal of Theoretical Biology **168**, 175 (1994).
[33] U. B. Kaupp and L. Alvarez, Eur. Phys. J-Spec. Top. **225**, 2119 (2016).
[34] P. Sartori, V. F. Geyer, A. Scholich, F. Jülicher, and J. Howard, eLife **5**, e13258 (2016).
[35] Y. Tu, Proc. Natl. Acad. Sci. USA **105**, 11737 (2008).
[36] P. Martin, A. J. Hudspeth, and F. Jülicher, Proc. Natl. Acad. Sci. USA **98**, 14380 (2001).
[37] K. Y. Wan and R. E. Goldstein, Phys. Rev. Lett. **113**, 238103 (2014).
[38] G. Quaranta, M. Aubin-Tam, and D. Tam, Phys. Rev. Lett. **115** (2015).
[39] G. Klindt, C. Ruloff, C. Wagner, and B. M. Friedrich, Phys. Rev. Lett. **117**, 258101 (2016).
[40] S. L. Tamm, Invertebr. Biol. **133**, 1 (2014).
[41] S. Nonaka, S. Yoshiba, D.Watanabe, S. Ikeuchi, T. Goto, W. F. Marshall, and H. Hamada, PLOS Biology **3**, e268 (2005).